ISABE-2015-20103

TRANSIENT PERFORMANCE SIMULATION OF AIRCRAFT ENGINE INTEGRATED WITH FUEL AND CONTROL SYSTEMS

Chen Wang **Yi-Guang Li**
School of Aerospace, Transport and Manufacturing, Cranfield University
Cranfield, Bedford MK43 0AL, UK

Bao-Ying Yang
Beijing HangKe Engine Control System Technology Co. Ltd., Changping, Beijing, 102200, China

ABSTRACT

A new method for the simulation of gas turbine fuel systems based on an inter-component volume method has been developed in this study. It is able to simulate the performance behaviour of each of the hydraulic components including pumps, valves, metering unit, etc. of a fuel system using physics-based models, which potentially offers more accurate results compared with those using transfer functions. A transient performance simulation system has been set up for gas turbine engines based on an inter-component volume (ICV) method. A proportional-integral (PI) control strategy is used for the simulation of engine control systems. An integrated engine and its control and hydraulic fuel systems has been set up to investigate their coupling effect during engine transient processes. The developed simulation method and the system have been applied to a model aero gas turbine engine to demonstrate the effectiveness of the method. The results show that the delay of the engine transient response due to the inclusion of the fuel system model is noticeable although relatively small. The developed simulation method is generic and can be applied to the performance simulation of any other gas turbines and their control and fuel systems.

NOMENCLATURE

A	Area (m^2)
B	Bulk Modulus (Pa)
Cd	Orifice Discharge Flow Coefficient
Cp	Specific Heat at Constant Pressure (J/kg.K)
CMF	Constant Mass Flow
$CPDV$	Constant Pressure Differential Valve
dm	Volume Stored Air Mass Variation
dP	Derivative of Pressure
dT	Derivative of Temperature
dV	Derivative of Volume
E	Energy (kJ)
e(t)	Controller Input Error
HPP	High Pressure Pump
I	Shaft Inertia
ICV	Inter-Component Volume
k	Valve Opening Area Coefficient
K_I	Integral Gain
K_P	Proportional Gain
LPP	Low Pressure Pump
m	Mass (kg)
MU	Metering Unit
P	Total Pressure (kPa)
PCN	Relative Rotational Speed
PR	Compressor pressure Ratio
PSP	Pump Shaft Power (W)
Q or Q_{ff}	Fuel Volumetric Flow Rate (m^3/s)
R	Gas Constant
SP	Engine Shaft Surplus Power (W)
T	Total Temperature (K)
T_i	Time Constant of Integral Action (s)
T_s	Time Constant of Sensor Delay (s)
TET	Turbine Inlet Temperature
u(t)	Controller Output Signal
V	Volume Chamber Volume (m^3)
Vs	Fuel Flow Speed (m/s)
W or W_{ff}	Fuel Mass Flow Rate (kg/s)
Δt	Calculation Step (s)

GREEK LETTERS

α	Thermal Expansion Coefficient (K^{-1})
η	Pump Efficiency
κ	Heat Producing Coefficient of Valve
κ_T	Isothermal Compressibility (Pa^{-1})
ρ	Density (kg/m^3)
ϕ	Thermal Energy (J)
Δ	Difference
∂	Partial Derivative

Subscripts

I	Integral
in	Component Inlet
out	Component Outlet
P	Proportional
P	Constant Pressure

T	Constant Temperature
p	Previous Calculation Step
c	Current Calculation Step
v	Constant Volume

INTRODUCTION

Performance simulations have been widely used in modern gas turbine engine designs in order to shorten design cycles and reduce development costs. Such simulations can be classified into design point, off-design steady state, and transient performance simulations depending on how the engines are operated. Engine transient performance simulation is very useful in the initial stage of engine development. For example, it will be able to assess the safety of transient operations of new engines including accelerations and decelerations, and to provide a numerical test-bed for the development of control systems including the investigation of the control system dynamic behaviour and the coupling between the engines and their control systems. However, it is found in the literature that fuel systems, as part of the fuel control and delivery systems have been ignored in gas turbine transient performance simulations.

An engine system, a controller, sensors, and a hydraulic fuel system are four basic elements of a gas turbine propulsion system. Most currently developed engine performance modelling systems, such as NPSS [1-3], C-MAPSS [4-5], Turbomatch [6-7], GasTurb [8-9], GSP [10], TERTS [11], etc. only focus on the simulation of engine systems and their controllers but ignore the sensors and actuators or treating them as first order lags [12]. Such simplification ignores the non-linear effect of these physical components and their impact on the whole propulsion systems and may cause noticeable prediction errors. In the operation of gas turbine propulsion systems, fuel flow rate injected into an engine combustion chamber is not only decided by the controller, but also affected by the execution of fuel control actuators including pumps, valves, and metering unit, etc. [13] Therefore, fuel output delay and fluctuation due to fuel system response will directly affect engine combustion and engine performance during transient processes.

An inter-component volume (*ICV*) method for gas turbine transient performance simulation was firstly introduced by Fawke and Saravanamuttoo [14-15]. A comparison of ICV method and a constant mass flow (CMF) method for engine transient simulation was also provided in [14]. Further simulation capability and computer software for both steady and transient performance simulations of gas turbines, such as DYNGEM by Sellers and Daniels [16], HYDES by Szuch [17] and GENENG by Koening and Fishbach [18] were also reported. At that time, both the ICV and the CMF methods had been thoroughly analysed and used for the steady and transient performance simulation of a variety of gas turbine engines.

In this paper, to investigate the performance behaviour and the effect of fuel system on engine transient behaviour, the ICV method [14-15] has been further developed and used in the performance simulation of control and hydraulic fuel systems. At the same time, a gas turbine transient performance simulation system based on the original ICV method and a hydraulic fuel system model based on the new ICV method has been developed. An integrated engine, control and hydraulic fuel system has been developed and used to simulate the performance behaviour of a model single-spool turbojet engine to demonstrate the effectiveness of the developed method. Results of a transient process of the model engine with and without the inclusion of the hydraulic fuel system have been simulated and compared with each other to illustrate the effectiveness of the fuel system model on engine transient performance simulation. Relevant discussions and conclusions are provided accordingly.

METHODOLOGY

Engine Transient Performance Simulation with Inter-Component Volume (ICV) Method

Engine transient performance simulation is used to investigate the engine dynamic behaviour from one steady state condition to another, such as that during acceleration or deceleration processes. Although the continuation of energy, mass and momentum is still satisfied, equilibrium of work, mass flow, and heat transfer within an engine system will be broken during a transient process, which is different from that at the steady state engine operating conditions. Two different transient performance simulation methods are available, one is the Continuous Mass Flow (*CMF*) method [19] and the other is the Inter-Component Volume (*ICM*) method [14-15]. In this study, the *ICV* method is used to simulate the transient behaviour of gas turbine engines.

Figure 1 shows a typical single-spool turbojet model engine used in this study. It consists of an intake, a compressor, a combustor, a turbine driving the compressor, and a nozzle. Working fluid is assumed to be air in cold sections and gas in hot sections of the model engine.

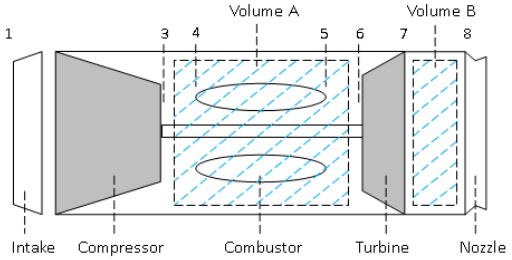

Figure 1: Schematic of Single-Spool Turbojet Model Engine Configuration

The following are three most important factors that have to be considered in transient performance simulation processes using the *ICM* method.

The first is the unbanlance of work between the components on the same shaft. For example, if the work produced by a turbine is more than the work consumed by a compressor, the engine will be driven into an acceleration process based on the rotordynamic equation represented by Equation (1)

$$\frac{dN}{dt} = \frac{60SP}{4\pi^2 IN} \qquad (1)$$

where N is the shaft rotational speed, I the shaft inertia and SP the surplus power which is the difference between the generated and consumed power.

The second is the consideration of volume dynamics in a volume between adjecent components where the mass flow going into the volume may be different from that going out of the volume causing accululation or dispersion of mass in the volume. Two inter-component volumes are shown in Figure 1 for the model engine, one is between the compressor and the turbine (Volume A) and the other is between the turbine and the nozzle (Volume B). Volume dynamics is represnted by Equation (2) where the change of volume pressure can be calculated by using the equation of state for perfect gas [14, 20].

$$dP = \frac{RT}{V} dm \qquad (2)$$

where P is the volume pressure, T the volume temperature, V the volume, m the air mass and R the universal gas constant.

The third factor is the fuel schedule provided by fuel control and fuel delivery systems. This will be discussed in more details in the next section.

More details of gas turbine transient performance simulation using the *ICM* method can be found in [20].

Engine Control System Simulation

The engine fuel control is a two-step process where three fuel schedules for steady state, acceleration and deceleration respectively have been used. These fuel schedules shown in Figure 2 provide required fuel flow rate W_{ff} signal to the fuel system based on the demand and measured engine relative rotational speed *PCN* that is the handle of the engine.

As shown in Figure 2, the steady state fuel schedule is the dash line. In order to keep an engine transient process quickly and safely, a minimum fuel selection logic called "Low Win Logic" and a maximum fuel selection logic called "High Win Logic" are embedded into the controller. At an initial phase of acceleration or deceleration, the schedule may predict a required fuel flow rate based on cockpit shaft speed command and the measured shaft speed. This predicted fuel flow rate may be larger than the value limited by the fuel selection logic. Therefore, fuel flow rate will be regulated by the fuel selection logic. When the engine approaches the desired end point of the transient process, fuel flow rate signal provided by the fuel schedule will become smaller than that estimated by the fuel selection logic. When that happens, the control process goes into second step and the controller will take over the fuel control until the engine reaches its desired steady state. The idea of the coupled two-step engine control and the fuel selection logic is represented in Figure 3.

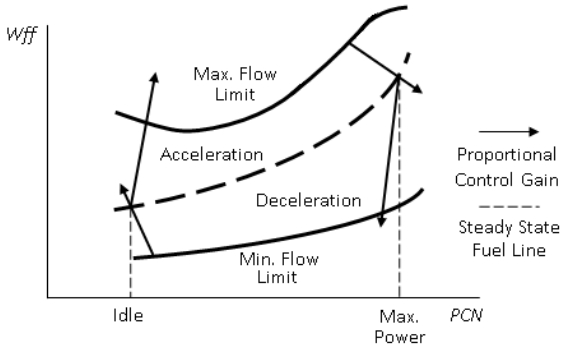

Figure 2: Fuel Schedule of Model Engine

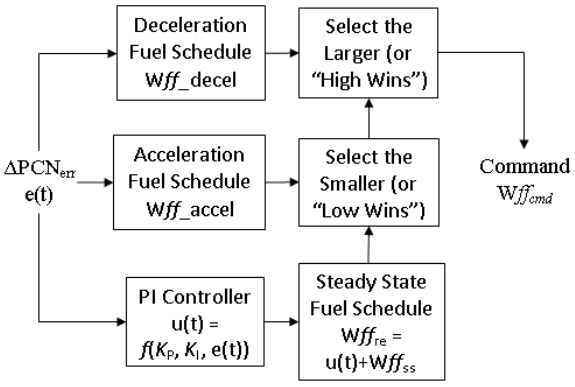

Figure 3: Diagram of Coupled Engine Controller and Fuel Selection Logic

A proportional-integral-derivative controller (PID controller) may be used in the second step of the fuel control process. It is a control loop feedback mechanism (controller) widely used in industrial control systems. It is historically been considered to be the most useful controller [21]. *PID* Controller aims to minimise the error value as the difference between the desired and monitored system variable by transferring the error into a controlled signal to govern the system operation. For a certain in-coming error signal, the *PID* control algorithm involved three actions: *P* (proportional) action is proportional to the present error, *I* (integral) action depends on the accumulation of past errors and *D* (derivative) action is a prediction of future

errors, based on current rate of change [22]. In this study, only *PI* controller is used for simplicity.

Equation (3) is the mathematical representation of the *PI* control algorithm [23]

$$u(t)=K_P e(t)+K_I \frac{1}{T_i}\int_0^t e(\tau)d\tau \quad \textbf{(3)}$$

where $u(t)$ is the control signal, $e(t)$ is the control error, K_P and K_I are the control gains of the proportional action and the integral action respectively, and T_i is a time constant of the integral action.

The *PI* control algorithm can also be shown graphically in Figure 4 where integral action is represented by a Laplace transfer function $\frac{1}{s}$. To implement a continuous-time control law in digital computer, the Laplace transform of integral action should be approximated through Z-Transform discretization. Thus, the *PI* algorithm in Figure 2 may be more conveniently represented by Equation (4).

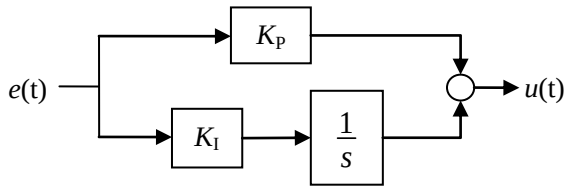

Figure 4: PI Controller Algorithm Diagram

$$u(t)=K_P\times e(t)+K_I\times\frac{T_i}{2}\times\frac{z-1}{z+1}\times e(t) \quad \textbf{(4)}$$

where T_i is equal to the calculation time step Δt.

Engine Fuel System Simulation

A fuel system is typically a hydraulic system and its function is to deliver required fuel flow to the engine combustion chamber to maintain the propulsion system operation. A typical fuel system is shown in Figure 5, which is consisted of a low pressure pump (LPP), high pressure pump (HPP), metering unit (MU), constant pressure differential valve (CPDV), throttle, injector, and tubes connecting these components.

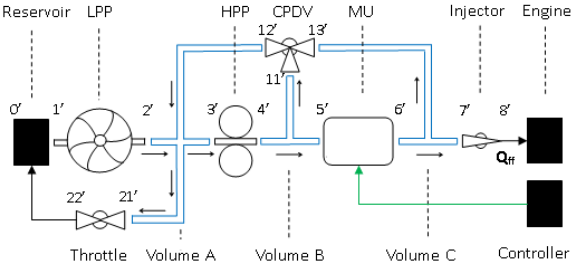

Figure 5: Schematic of Engine Fuel System

In the fuel system shown in Figure 3, three tubes connect different fuel system components. Fuel sucked from an oil reservoir is firstly pumped through the low pressure pump (LPP) that deliver the fuel to the high pressure pump (HPP) with a proper fuel pressure to avoid fuel vaporization. The high pressure pump is used to pressurize the fuel further to ensure it has sufficient pressure to be injected into the engine combustion chamber. The fuel flow rate metered at a metering unit (MU) is the function of both the opening area and the pressure drop across the MU. If the pressure drop across the MU is maintained constant, the fuel flow rate becomes only proportional to the MU orifice opening area that can be adjusted by the controller.

As the LPP outlet pressure has a significant impact on the LPP volume flow rate, a throttle is added to release the over-pumped fuel back into the reservoir to avoid pressure accumulation in the pipe.

Inter-Component Volumes (ICM) Method

Fuel system components are connected by tubes or ducts, named as inter-component volumes, filled with pressureized fuel fluid. During a transient process, the pressure inside the volume may vary due to the inconsistent fuel flow entering and leaving the volume. The *ICV* method [20] is based on such a phenomenon and has been effectively developed and used in gas turbine transient performance simulation where the working fluid is either air or gas being compressible and perfect gas. In this study, it is the first time that the *ICV* method is introduced into the performance simulation of a hydraulic fuel system where the working fluid is fuel being incompressible. To assist the understanding of the *ICV* method, a typical inter-component volume may be schematically represented by Figure 6.

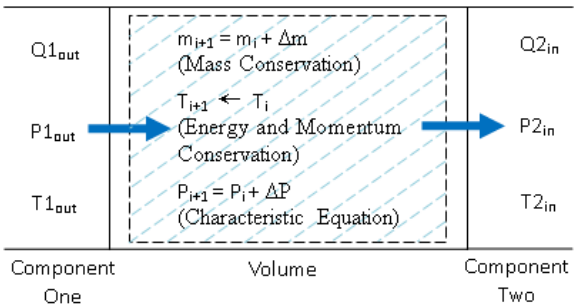

Figure 6: Inter-Component Volume

It is assumed that the system running time is first divided into a series of calculation time steps. The varying system state is then calculated at each small time step during which the system is regarded as pseudo-steady and the transient process is calculated from one step to the other until the system reaches its aimed steady state.

Volume state variation is governed by the conservation of mass, energy and momentum. The conservation of mass is represented by Equations (5)

$$m_{i+1} = m_i + (\sum W_{i_{in}} - \sum W_{i_{out}}) \times \Delta t \quad \textbf{(5)}$$

where m is the mass inside the volume, W is the fuel mass flow rate, Δt is the time step, subscript i represents current time moment, $i+1$ represents the next time moment, in is the volume inlet flow, and out is the volume outlet flow. In the fuel system, volumetric flow rate Q instead of mass flow rate W is normally used to represent the fuel flow rate because the metering unit only meters fuel volumetric flow. The fuel mass flow rate W can be calculated by Equation (6).

$$W = \rho \times Q \quad \textbf{(6)}$$

where ρ is the fuel density. The conservation of energy is represented by Equation (7)

$$T_{i+1} = \frac{\sum E_{i_{in}} + E_i - \sum E_{i_{out}} - \frac{1}{2} m_i Vs_i^2}{m_{i+1} Cp_{i+1}} \quad \textbf{(7)}$$

where T is the volume temperature, E the fuel flow energy and Vs is the fuel flow velocity. The energy item E in Equation (7) includes static and dynamic energy of the fuel flow that can be calculated by Equation (8).

$$E = m \times Cp \times T + \frac{1}{2} m \times Vs^2 \quad \textbf{(8)}$$

In each volume, both inlet and outlet flow velocity can be calculated by Equation (9)

$$Vs = Q / A \quad \textbf{(9)}$$

where A is the volume cross area. The conservation of momentum is represented by Equation (10).

$$Vs_{i+1} = \frac{\sum (m_i Vs_i)_{in} + (m_i Vs_i) - \sum (m_i Vs_i)_{out}}{m_{i+1}} \quad \textbf{(10)}$$

To ensure these conservation laws are used correctly, the following three assumptions are made:

- The fuel entering the volume will be fully mixed immediately with the fuel already in the volume;
- The status of the fuel within a volume is kept unchanged within a time step;
- The fuel flow within a volume experiences an isentropic process.

The isothermal compressibility κ_T shown in Equation (11) is introduced [24] in this study.

$$\kappa_T = -\frac{1}{V}\left(\frac{\partial V}{\partial P}\right)_T \quad \textbf{(11)}$$

where κ_T is a pressure coefficient to measure fluid volume variation due to pressure change under constant temperature. Equation (12) based on the equation of state for incompressible flow is used to represent the pressure variation within a volume affected by both temperature and volume change.

$$dP = \frac{\alpha}{\kappa_T} dT - \frac{1}{V \kappa_T} dV \quad \textbf{(12)}$$

where α is a temperature coefficient to measure how the fluid volume is affected by the temperature change under constant pressure. As both α and κ_T are derived from the same equation of state of fluid, it is not easy to specify these two coefficients' values accurately at the same time when the pressure variation needs to be calculated. To simplify the calculation, the temperature variation due to the fuel fluid compression or expansion in each calculation step is ignored and therefore the pressure variation within a volume is only affected by the fluid volume variation.

In addition, "bulk modulus" B is introduced to measure the resistance of a fluid to compression or expansion and it is defined as the ratio of pressure stress to volumetric strain. The "bulk modulus" is the function of fluid pressure at certain temperature [25] shown in Equation (13) [24].

$$B = \frac{1}{\kappa_T} = -V\left(\frac{\partial P}{\partial V}\right)_T \quad \textbf{(13)}$$

Therefore the volume pressure change dP produced by the fluid volume change dV can be estimated by Equation (14) when the temperature variation is ignored.

$$dP = -\frac{B}{V} \times dV \quad \textbf{(14)}$$

where V is the volume chamber volume, and dV is given by Equation (15).

$$dV = \sum Q_{in} - \sum Q_{out} \quad \textbf{(15)}$$

Therefore, the new volume pressure produced at next time step P_{i+1} is then calculated by Equation (16).

$$P_{i+1} = P_i + dP \quad \textbf{(16)}$$

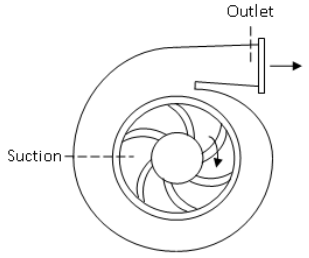

Figure 7: Schematic of Centrifugal Pump

Pumps

Pumps are used to pressurize fuel flow in order that it can be transported and injected into the engine combustion system. Two types of pumps, i.e. centrifugal pumps as low pressure pumps and gear pumps as high pressure pimps are normally used in hydraulic fuel systems and the schematics of them are represented in Figures 7 and 8 respectively.

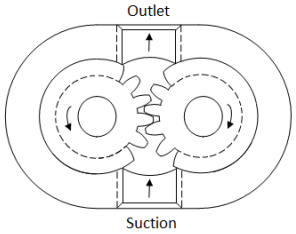

Figure 8: Schematic of Gear Pump

In this study, empirical pump characteristic maps are used to describe the performance behaviour of the pumps. The maps may be obtained in pump rig tests and are assumed to be available. Four characteristic parameters including shaft speed PCN , volumetric flow rate Q , efficiency η, and pressure increase ΔP are used to describe the pump characteristics in the maps. When any two of the characteristic parameters are given, the other two parameters can be obtained easily through the interpolation of the maps. Figures 9 and 10 show typical characteristic maps for centrifugal pumps and gear pumps, respectively.

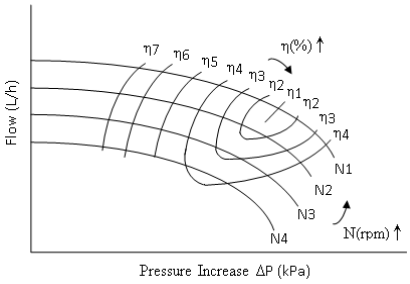

Figure 9: Typical Centrifugal Pump Characteristic Map

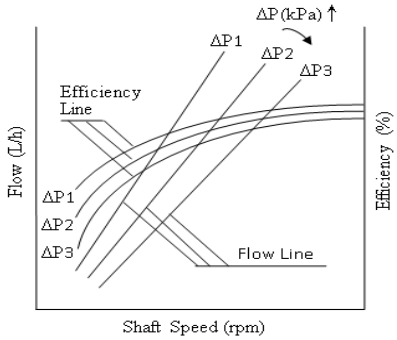

Figure 10: Typical Gear Pump Characteristic Map

As pumps are directly connected to engine shaft and are driven by an engine, pump shaft rotational speed is assumed to be equal to the engine shaft speed and there is no time delay between engine and pump shaft speeds during engine transient processes.

The energy transformed to the fuel flow through pump can be divided into two parts, one is used to pressurise the fuel flow and the other is to increase fuel temperature by assuming the pump is an adiabatic system. In other words, pump shaft power (PSP) can be obtained by Equation (17) [26].

$$PSP = \frac{\Delta P \times Q}{\eta} \qquad \textbf{(17)}$$

The thermal energy ϕ absorbed by the fuel flow can be calculated by Equation (18) [27].

$$\phi = PSP \times (1 - \eta) \qquad \textbf{(18)}$$

Therefore, the temperature rise ΔT of the fuel flow can be then calculated by Equation (19).

$$\Delta T = \frac{\phi}{W \times Cp} \qquad \textbf{(19)}$$

where Cp is the specific heat of the fuel.

Valves

Valves are the devices to regulate and control fuel flow rate in the system. By controlling the opening and closing of a valve, the fuel flow rate can be controlled.

A constant pressure differential valve (CPDV), a schematic of it shown in Figure 11, is a device to maintain a constant pressure drop across a fuel metering unit (MU). It has two inlet ports, one connecting the HPP outlet and the MU inlet and the other connecting the MU outlet. It has an exit port where fuel will be bypassed from the inlet of the MU to the entry of HPP via a cone valve in order to keep constant pressure drop. Inside the CPDV, a film connecting with a pressurized spring is installed to separate the CPDV into two independent chambers where pressure difference can be transferred but fuel cannot be. The pressure drop is balanced by the spring whose movement adjusts the opening area of valve orifice.

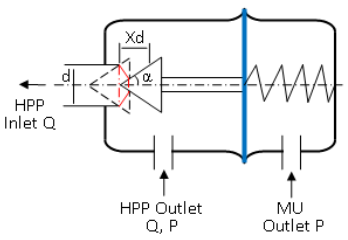

Figure 11: Schematic of constant pressure differential valve (CPDV)

A metering unit is the device to meter the engine required fuel flow rate based on the controller order. A typical metering unit is consisted of a stepper motor, a rack and pinion mechanism, and a metering valve. A schematic of a metering unit valve is represented in Figure 12.

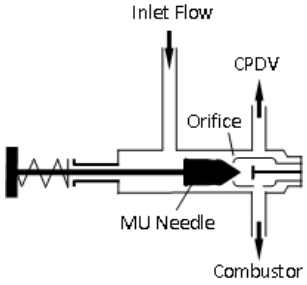

Figure 12: Schematic of metering unit valve

A throttle is the device to constrict or obstruct the fuel flowing through it. This component is to bypass the fuel flow at HPP inlet to the fuel reservoir to ensure no significant pressure rise between the LPP and the HPP.

An injector is to deliver the metered fuel into engine combustor. To ensure the fuel is burned efficiently, liquid fuel is mixed with air inside the injector and the fuel/air mixture is injected into the engine combustor. A schematic of an injector is shown in Figure 13.

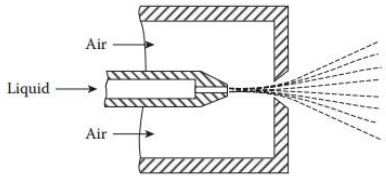

Figure 13: Schematic of Fuel Injector [29]

Despite different configurations and working principle of different valves, valve performance is mainly determined by the orifice performance.

The MU and the CPDV are able to change the orifice area depending on fuel flow demand. For these components, the orifice area is determined by the pressure drop across the orifice and the required volume fuel flow rate so it can be estimated by Equation (20).

$$A = \frac{Q}{C_d} \times \sqrt{\frac{\rho}{2\Delta P}} \qquad \textbf{(20)}$$

where C_d is the orifice discharge flow Coefficient, Q the volumetric flow rate, ρ the fuel density and ΔP the pressure difference across the orifice. The required orifice area can be obtained by moving the accessary mechanism and the moving distance ΔXd may be estimated by Equation (21) when the required change of opening areas ΔA_c of an orifice becomes available.

$$\Delta Xd = \Delta A_c / k \qquad \textbf{(21)}$$

where k is the valve opening area coefficient to the opening position Xd .

For the throttle and the injector whose orifice areas are fixed, the fuel volumetric flow rate through the orifice can be calculated by Equation (22) [26].

$$Q = Cd \times A \times \sqrt{\frac{2\Delta P}{\rho}} \qquad \textbf{(22)}$$

The thermal energy ϕ absorbed by the fuel flow passing through the orifice may be estimated by Equation (23) [27].

$$\phi = \kappa \times \Delta P \times Q \qquad \textbf{(23)}$$

where κ is heat producing coefficient of the valve. By using Equation (19), the fuel flow temperature rise across valve orifice can be calculated.

Integrated Engine, Control and Fuel System

With the models for all the fuel system components become available, an integrated fuel system performance model has been set up. Figure 14 shows the calculation flow chart for the fuel system represented in Figure 3. The fuel system calculation process follows the fuel flow path in the system starting from the LPP. For each calculation time step, if a required parameter of a component is not coming from its upstream component but from its down-steam component, the value of this parameter will be inherited from the last step calculation. For example, both the LPP and the HPP pumps need the pump pressure increase as inputs, they are calculated using the inlet pressures at current time and the outlet pressures at previous time step. The volumetric flow rate Q through each orifice of the throttle, injector, metering unit and constant pressure differential valve is estimated from the orifice area A and pressure drop across it. Temperature increase through the orifice can also be estimated from its thermal equation.

The integrated engine, fuel and control system has been established and shown in Figure 15. In this integrated system model, the gas turbine drives the fuel system via a shaft connection. Therefore, the shaft power surplus SP in Equation (1) can be obtained by Equation (24).

$$SP = TW - CW - \sum PSP \qquad \textbf{(24)}$$

Where TW is the turbine power output, CW is the compressor power consumption and PSP is the pump power consumption. It is assumed that only the pump power consumption is considered in the fuel system.

Engine shaft speed is measured by a speed sensor and the measured signal is transmitted to the engine

controller with a first order lag $\frac{1}{T_s s+1}$. The controller receives the measured speed signal and speed demand indicated by a cockpit power level angle (*PLA*) to calculate the required fuel flow rate Q_{ff} using the *PI* control schedule. Q_{ff} is then turns into the movement ΔXd of the mechanism in the fuel system to adjust the orifice opening area of the metering unit. The metered fuel flow rate W_{ff} from the fuel system will then be injected into the engine combustion chamber to maintain the engine operation.

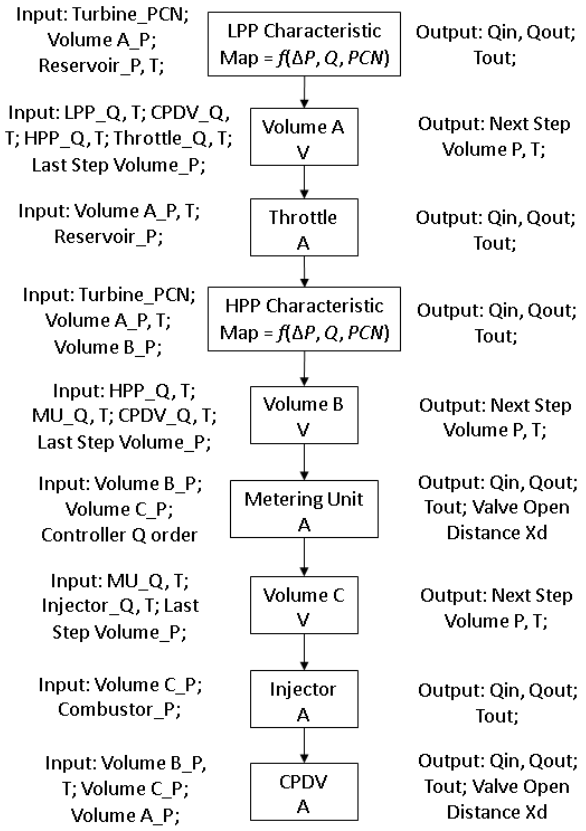

Figure 14: Flow Chart of Fuel System Model

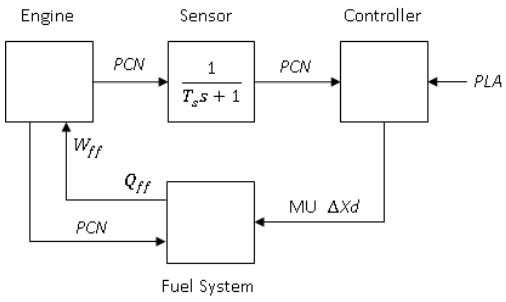

Figure 15: Schematic of Integrated Engine, Control and Fuel System

APPLICATION AND ANALYSIS

Model Engine

The developed integrated engine, control and fuel system transient performance simulation method has been applied to a model aircraft gas turbine engine shown in Figure 1. Two inter-component volumes are included in the transient engine performance model, one located between the compressor and the turbine and the other between the turbine and the nozzle. Spool relative rotational speed *PCN* is chosen as the handle and is controlled by the controller to determine the operating condition of the engine. Table 1 lists the engine performance specification at *ISA* sea level static condition and the key performance parameters used in the performance modelling.

Table 1: Engine Performance Specification at Design Point and Key Parameters

Parameters	Value
Air Flow Rate (kg/s)	77.2
Compressor Pressure Ratio	8.8
Compressor Isentropic Efficiency	0.84
Combustion Efficiency	0.99
Volume A (m^3)	0.8
Turbine Entry Temperature (TET) (K)	1141
Turbine Isentropic Efficiency	0.87
Volume B (m^3)	0.2
Thrust (kN)	41.43
SFC (g/kN.s)	31.4

Model Fuel System

The model fuel system used in this study for the model engine is shown in Figure 2. Table 2 lists key parameters of the model fuel system.

Table 2: Fuel System Parameters at Design Point

Component		Value
Low Pressure Pump	Fuel Flow Rate (L/h)	8643.6
	Pressure Rise (kPa)	600
	Efficiency	0.6
Volume A	Volume (m^3)	0.1
Throttle	Fuel Flow Rate (L/h)	8000
High Pressure Pump	Fuel Flow Rate (L/h)	9300
	Pressure Rise (kPa)	3500
	Efficiency	0.8
Volume B	Volume (m^3)	0.1
Metering Unit	Fuel Flow Rate (L/h)	5762.4
	Pressure Drop (kPa)	400
	Opening Coefficient	0.009
Volume C	Volume (m^3)	0.05
Injector	Fuel Flow Rate (L/h)	5762.4
	Area (mm^2)	30.5

The characteristic map shown in Figure 16 is for the centrifugal pump and the map shown in Figure 17 is for the gear pump. The efficiency of each pump is assumed to be constant for simplicity as it normally changes very little. The developed ICV method described in earlier part of the paper was applied to the fuel system for its transient performance simulation. The control gains of the PI controller are given in Table 3. In practice, the determination of the fuel schedule should consider keeping enough safety margin for compressor surge, turbine over-heating, shaft over-speeding, combustor blow out, etc., which are not rigorously considered in this study.

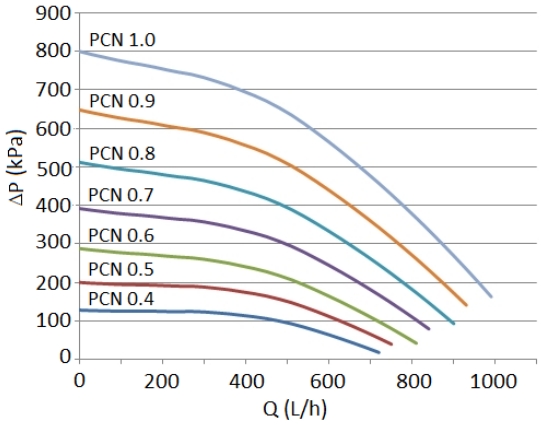

Figure 16: Characteristic Map of Centrifugal Pump

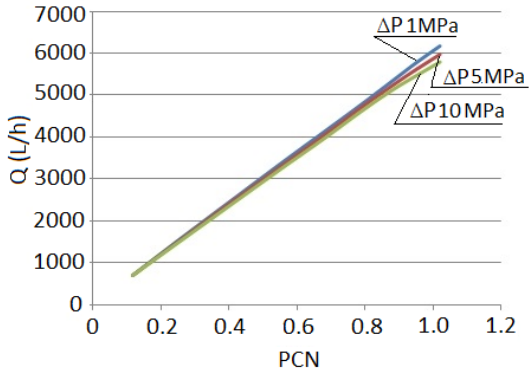

Figure 17: Characteristic Map of Gear Pump

Table 3: PI Controller Gains

Proportional Gain K_P	20
Integral Gain K_I	0.001

Engine Transient Performance Simulation Results

The transient performance of the model engine has been simulated using the integrated engine, control and fuel system shown in Figure 13. It is assumed that the model engine is running at an altitude of 1000 m and at Mach number 0.5. It is also assumed that the engine starts acceleration from its steady state condition at PCN of 0.7, accelerates to its maximum power at PCN of 1.0, stays at the maximum condition for about 20 seconds and then decelerates back to the PCN of 0.7.

Figure 18 shows the PNC command signal against the actual PCN variation during the whole transient process of 70 seconds. Compared with the command signal, the delay of the actual PCN response is due to the transient response of the engine and its control and fuel systems.

Figure 19 shows a comparison between the fuel command signal provided by the fuel selection logic and the actual fuel flow rate delivered by the control and fuel system over time. It can be seen that during the acceleration process the delivered fuel flow rate follows the fuel schedule initially and then deviates from the fuel schedule at about 15 seconds. This is because the fuel controller takes over the fuel control task and controls the fuel flow rate based on the difference between the desired and actual engine shaft speed *PCN*. Similar phenomenon can be observed during the deceleration process where the fuel flow rate follows the fuel schedule until at around 56 seconds and then the controller takes over the fuel control until the engine reaches its desired end steady state condition.

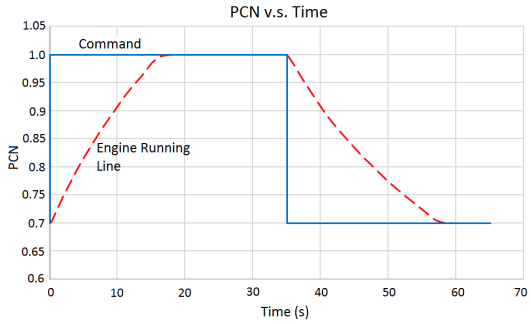

Figure 18: Model Engine PCN v.s. Time at Altitude = 1000m, Mach = 0.5

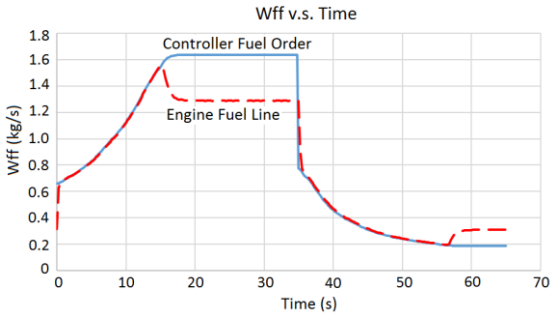

Figure 19: Model Engine Wff v.s. Time at Altitude = 1000m, Mach = 0.5

Figure 20 shows a comparison of the trajectories of actual fuel flow variation against those from the fuel schedule for the acceleration and the deceleration processes. They are also compared with the engine fuel flow rate at steady state conditions.

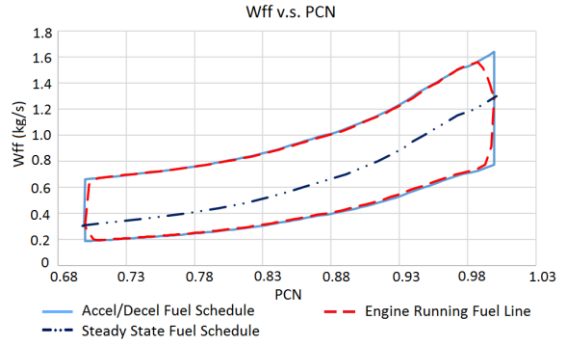

Figure 20: Model Engine Wff v.s. PCN at Altitude = 1000m, Mach = 0.5

To demonstrate the impact of the inclusion of the fuel system model in the engine transient performance simulation, a comparison of the simulated transient process with and without the fuel system model is made in the following. For the same transient process of acceleration and deceleration just described above, the fuel flow rate variations of the model engine is shown in Figure 21 where the delayed transient response by about 0.5 second due to the inclusion of the fuel system model is obvious. The most significant delays happen at the points where the fuel flow control is switched between the fuel schedule and the fuel controller. This is due to the delay caused by the action of the fuel system components and the effect of the inter-component volume.

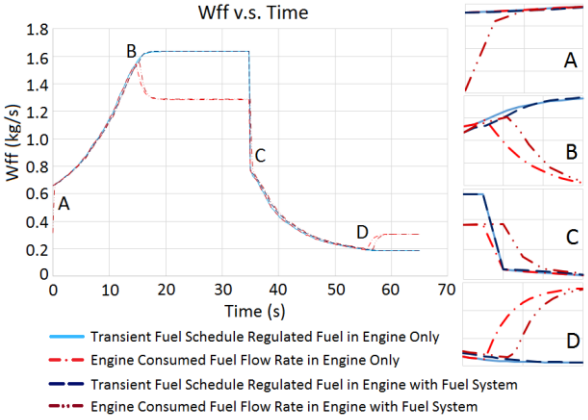

Figure 21: Transient Fuel Schedules Comparison of Engine with and without Fuel System

More engine parameters, such as *PCN*, *TET*, and compressor exit pressure P_3 varying over time for the same transient process are also shown in Figures 22 to 24. It can be seen in the figures that the predicted variation of these parameters with and without the inclusion of the fuel system model follow the same pattern as that shown in Figure 21 and the differences are small.

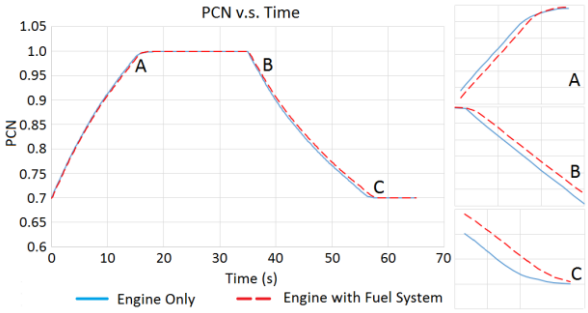

Figure 22: Engine Relative Rotational Speed PCN Comparison for Engine with/without Fuel System

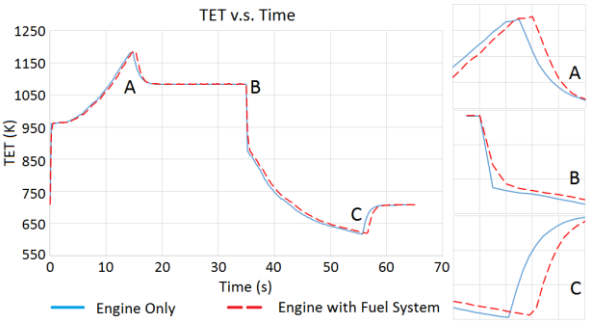

Figure 23: Turbine Inlet Temperature TET Comparison for Engine with and without Fuel System

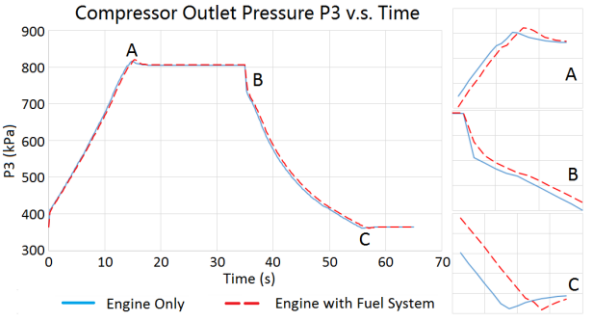

Figure 24: Compressor Outlet Pressure P_3 Comparison for Engine with and without Fuel System

CONCLUSIONS

A novel transient performance simulation method for engine hydraulic fuel system based on an inter-component volume (ICV) method has been introduced in this paper. It allows physics-based simulation models to be built up for gas turbine engines with the inclusion of control and fuel systems, which is potentially more accurate than the methods using transfer functions. The coupling effect between a model gas turbine engines and its control and fuel system during engine transient processes has also been investigated. The developed ICV-based fuel system simulation method has been successfully applied to the performance simulation of the transient process of a model aero gas turbine engine where acceleration and

deceleration process of the model engine are simulated and demonstrated. The simulated results and their comparison show that the fuel flow delay during the transient process due to the inclusion of fuel system model and the effect of inter-component volume is around 0.5 second and is noticeable in the process when the fuel control is switched between the fuel schedule and the fuel controller but such delay is relatively small.

REFERENCES

1. Lytle J K (1999), "The Numerical Propulsion System Simulation: A Multidisciplinary Design System for Aerospace Vehicles", NASA/TM - 209194.
2. Lytle J K (2000), "The Numerical Propulsion System Simulation: An Overview", NASA/TM - 209915.
3. Naiman C G, Follen G J (2001), "Numerical Propulsion System Simulation – A Common Tool for Aerospace Propulsion Being Developed", NASA/TM – 210605.
4. May R D, Csank J, Lavelle T M, Litt J S, and Guo T H (2010), "A High-Fidelity Simulation of a Generic Commercial Aircraft Engine and Controller", AIAA-2010-6629, 46th AIAA/ASME/SAE/ASEE Joint Propulsion Conference and Exhibit, 25-28 July 2010, Nashville, TN.
5. Frederick D K, DeCastro J A, Litt J S (2007), "User's Guide for the Commercial Modular Aero-Propulsion System Simulation (C-MAPSS)", NASA/TM – 215026.
6. Palmer J R (1967) "Turbocode Scheme for the Programming of the Thermodynamic Cycle Calculations on an Electronic Digital Computer", COA/AERO-198, College of Aeronautics, Cranfield Institute of Technology
7. Palmer J R, Pachidis V (2005), "The Turbomatch Scheme; for Aero/Industrial Gas Turbine Engine Design Point/Off Design Performance Calculation", Manual, Cranfield University, UK.
8. Kurzke J (1995), "Advanced User-Friendly Gas Turbine Performance Calculations on a Personal Computer", *ASME conference in Houston, TX, USA*, ASME 95-GT-147.
9. GasTurb web site "http: //www.gasturb.de".
10. Visser W P J, Broomhead M J (2000) "GSP, a generic object-oriented gas turbine simulation environment", NLR-TP-2000-267, National Aerospace Laboratory, NLR.
11. Visser W P J, Broomhead M J, van der Vorst J (2002), "TERTS, a generic real-time gas turbine simulation environment" NLR-TP-2002-069, NLR.
12. Jaw L C, Mattingly J D (2009), "Aircraft Engine Controls: Design, System Analysis, and Health Monitoring", AIAA 1801 Alexander Bell Drive, Suite 500 Reston, VA 20191-4344, USA.
13. US Department of Transportation (1976) "Airframe & Powerplant Mechanics: Powerplant Handbook"
14. Fawke A J, Saravanamuttoo H I H (1971), "Digital Computer Methods for Prediction of Gas Turbine Dynamic Response", Society of Automotive Engineers Rept. 710550.
15. Fawke A J (1970), "Digital Computer Simulation of Gas Turbine Dynamic Behaviour", Ph.D. Thesis, University of Bristol.
16. Sellers J F, Daniele C J (1975), "DYNGEM. A Program for Calculating Steady State and Transient Performance of Turbojet and Turbofan Engines", NASA TN D-7901.
17. Szuch J R (1974), "HYDES. A Generalized Hybrid Computer Program for Studying Turbojet or Turbofan Engine Dynamics", NASA TM X-3014.
18. Koening R W, Fishbach L H (1972), "GENENG. A Program for Calculating Design and Off-Design Performance for Turbojet and Turbofan Engines", NASA TN D-6552.
19. Larrowe V L, Spencer M M, Tribus M (1957), "A Dynamic Performance Computer for Gas Turbine Engines", Transactions A.S.M.E. October.
20. Rahman N U, Whidborne J F (2008), "A Numerical Investigation into the Effect of Engine Bleed on Performance of a Single-Spool Turbojet Engine", *Journal of Aerospace Engineering*, Volume 222, Number 7, pp. 939-949.
21. Benner S (1993), "A History of Control Engineering", IET.
22. Wikipedia http://en.wikipedia.org/wiki/PID_controller .
23. Astrom K, Hagglund T (1995) "Controllers: Theory, Design and Tuning", 2nd Edition, ISBN 1-55617-516-7.
24. Mastsuoka H, "Isobaric Thermal Expansion and Isothermal Compression", Illinois State University, Thermal Physics.
25. Coordinating Research Council (1983) "Hand Book of Aviation Fuel Properties", pp. 84-87, Society of Automotive Engineers, Inc. Warrendale, Pennsylvania.
26. Fan S Q, Li D, Fan D (2008), "Aero-engine Control on the Book", ISBN 9787561221617, CHINA.
27. Pu Z L (1983), "Aircraft Pump Design [M]", Academic Press, 12: 7-132.
28. Wei Y Y, Wang H Y, Miao W B (2014), "Analysis on Modeling of Constant Pressure Difference Valve for a Turboshaft Engine[J]" Aeroengine.2014.40(4): pp. 75-78.
29. Arthur H L, Dilip R B (2010), "Gas Turbine Combustion: Alternative Fuels and Emissions", Third Edition, CRC Press, ISBN 9781420086041, pp. 242-249.